Parameters of a runaway electron avalanche

E. V. Oreshkin,[1,a)] S. A. Barengolts,[1,2] V. I. Oreshkin,[3,4] and G. A. Mesyats[1]
[1]*P. N. Lebedev Physical Institute, RAS, Moscow, Russia*
[2]*A. M. Prokhorov General Physics Institute, RAS, Moscow, Russia*
[3]*Institute of High Current Electrons, SB, RAS, Tomsk, Russia*
[4]*Tomsk Polytechnic University, Tomsk, Russia*

(Received 17 June 2017; accepted 1 September 2017; published online 21 September 2017)

The features of runaway electron avalanches developing in air at different pressures are investigated using a three-dimensional numerical simulation. The simulation results indicate that an avalanche of this type can be characterized, besides the time and length of its exponential growth, by the propagation velocity and by the average kinetic energy of the runaway electrons. It is shown that these parameters obey the similarity laws applied to gas discharges. *Published by AIP Publishing.*
[http://dx.doi.org/10.1063/1.4990729]

I. INTRODUCTION

Runaway electrons (REs) were first detected in high-pressure gas discharges due to the x-rays generated in the discharge region.[1–3] Subsequently, REs were found in lightning discharges.[4,5] In 1992, the phenomenon called runaway electron breakdown (REB) was predicted.[6] It is supposed that REBs occur in high-altitude atmospheric discharges,[7,8] which are observed in the thunderstorm atmosphere at altitudes of 15–70 km from the Earth surface. The development of an REB is supposedly dominated by the avalanche of runaway electrons initiated by cosmic rays.[6] This supposition is confirmed by experimental studies.[7,8] REBs typically develop at low electric fields. For instance, an REB can develop in air at atmospheric pressure at an electric field of 2–3 kV/cm,[9] whereas a static breakdown occurs at an electric field $E_{\mathrm{br}} \sim 30$ kV/cm.[10]

The proposed existence of REBs provoked an active interest in REs, which have been extensively studied both theoretically[9,11–20] and experimentally.[21–27] For instance, discharges with $E_{av} \gg E_{br}$, where E_{av} is the average electric field in the electrode gap, were investigated experimentally.[21] It was revealed that in discharges of this type, the runaway electron signal waveform consists of a portion with a pronounced maximum, whose duration is several tens of picoseconds, and a tapered plateau of duration over 100 ps, which is supposedly related to an RE avalanche.

The occurrence of runaway electrons in a material immersed in an electric field is associated with a decrease in the braking force acting on an electron with increasing its energy. For a gas, the braking force acting on an electron due to inelastic loss with a transferred energy not above ε_1 can be described as[28]

$$F(\varepsilon_1) = \frac{2\pi e^4 Z n}{mv^2} \ln\left(\frac{2mv^2\varepsilon_1}{J^2}\right), \tag{1}$$

where v, e, and m are the electron velocity, charge, and mass, respectively; Z, n, and J are the nuclear charge, the atomic density of the gas, and the mean energy of inelastic loss in the gas, respectively. As an electron can lose all its energy in collisions, then for $\varepsilon_1 = \varepsilon_k$, where ε_k is the kinetic energy of the electron, expression (1) will describe the total braking force acting on the electron. The braking force depends on the gas species and is directly proportional to the gas pressure p. If the gas is a mixture of species, the total braking force is the sum of the braking forces for the species.

The braking force has a maximum in the range of low (nonrelativistic) electron energies and a minimum in the range of ultrarelativistic energies. In view of the relativistic relationship between the kinetic energy of an electron and its velocity, $\varepsilon_k = \frac{mc^2}{\sqrt{1-\frac{v^2}{c^2}}} - mc^2$, formula (1) can be rewritten as

$$F(\varepsilon_k) = \frac{2\pi e^4}{mc^2} Z n \frac{(\varepsilon_k + mc^2)^2}{\varepsilon_k^2 + 2mc^2\varepsilon_k} \ln\left(\frac{2mc^2}{J^2}\frac{\varepsilon_k^3 + 2mc^2\varepsilon_k^2}{(\varepsilon_k + mc^2)^2}\right). \tag{2}$$

To find the extreme points, we differentiate relation (2) with respect to ε_k and equate the derivative to zero. As a result, we obtain the transcendental equation

$$2mc^2 \ln\left(\frac{2mc^2}{J^2}\frac{\varepsilon_k^3 + 2mc^2\varepsilon_k^2}{(\varepsilon_k + mc^2)^2}\right) = 3\varepsilon_k + 4mc^2. \tag{3}$$

In the nonrelativistic limit, at $\varepsilon_k \ll mc^2$, Eq. (3) becomes $\ln\left(\frac{2\varepsilon_k}{J}\right) \approx 1$, from which we obtain the following expression for the position of the braking force maximum ($F_{\max}$): $\varepsilon_{\max} \approx \frac{2.718}{2} J$. Thus, in nitrogen, for which $J \approx 80$ eV, the electrons with energy $\varepsilon_k = \varepsilon_{\max} \approx 110$ eV will experience the greatest inelastic losses, as the braking force for them is a maximum. To the maximum braking force, there corresponds the electric field[10]

$$E_{cr} = \frac{F(\varepsilon_{\max})}{e} \approx \frac{4\pi e^3 Z n}{2.718 J}. \tag{4}$$

This electric field is called critical because, as soon as it is reached, all electrons in the gas become permanently accelerated. However, for runaway electrons to occur in a

a)E-mail: oreshkin@lebedev.ru

gas, the condition $E \geq E_{cr}$ should not necessarily be satisfied. In the range $E_c < E < E_{cr}$, where E_c is the electric field corresponding to the minimum braking force, an electron should have energy $\varepsilon_k \geq \varepsilon_k^{\min}$ to become permanently accelerated in a constant electric field of strength E. In the nonrelativistic limit, the minimum electron energy is determined by the formula

$$E = \frac{2\pi e^3}{\varepsilon_k^{\min}} Zn \ln\left(\frac{2\varepsilon_k^{\min}}{J}\right). \tag{5}$$

The braking force minimum is due to relativistic effects. It is well known that a fast electron interacts with the electrons and nuclei of gas atoms like with free particles. Therefore, at moderate energies (0.1–0.5 keV), the braking force decreases due to the decrease in Coulomb cross section with an increase in the velocity of the incident electron. For relativistic electrons, the velocity stops increasing with energy (it approaches the velocity of light), and the braking force increases logarithmically. We estimate the electron energy corresponding to the braking force minimum using relation (3). In the ultrarelativistic limit of $\varepsilon_k \gg mc^2$, relation (3) becomes $2mc^2 \ln\left(\frac{2mc^2\varepsilon_k}{J^2}\right) \approx 3\varepsilon_k$, from which we obtain

$$\varepsilon_{\min} \approx \frac{4}{3} mc^2 \ln\left(\frac{2mc^2}{J}\right). \tag{6}$$

Then to the minimum braking force, there corresponds the electric field

$$E_c = \frac{F(\varepsilon_{\min})}{e} \approx \frac{4\pi e^3 Zn}{mc^2} \ln\left(\frac{2mc^2}{J}\right). \tag{7}$$

This is a threshold electric field, such that both runaway electrons can occur and RE avalanches can develop in fields of strength $E > E_c$, whereas electrons do not "run away" in fields of strength $E \leq E_c$. Below, the development of runaway electron avalanches in air at different pressures and electrostatic fields is investigated based on numerical calculations. The acceleration of electrons under the action of a constant electrostatic force is simulated in a three-dimensional geometry.

II. SIMULATION OF THE FORMATION OF AN RE AVALANCHE

The 2D simulation of RE avalanches[29,30] was extended to a 3D geometry. The 3D numerical simulation is based on the Monte Carlo technique. The main equation describes the variation of the momentum of an electron in a constant electric field **E**:

$$\frac{d\mathbf{p}}{dt} = e\mathbf{E} - \mathbf{F}(\varepsilon_k) - (\Delta\mathbf{p})_{el}, \tag{8}$$

where $\mathbf{p} = \frac{m\mathbf{v}}{\sqrt{1-\frac{v^2}{c^2}}}$ is the electron momentum, c is the velocity of light in vacuum, and $(\Delta\mathbf{p})_{el}$ is the variation of the electron momentum due to elastic scattering. Three components of the momentum are calculated: p_x and p_y, both normal to the vector **E**, and p_z parallel to **E**.

The braking force in (8) is broken up into two terms as

$$\mathbf{F}(\varepsilon_k) = \sum_a \frac{2\pi e^4 Z_a n_a}{mv^2} \ln\left(\frac{2mv^2\varepsilon_k^{\min}}{J_a^2}\right)\frac{\mathbf{v}}{v} + \mathbf{F}_{es}. \tag{9}$$

The summation in (9) is performed over the gas species.

The first term describes a braking even in which an electron gives up an energy $< \varepsilon_k^{\min}$, which is too low for REs to occur. The second term $|F_{es}| = \sum_a \frac{2\pi e^4 Z_a n_a}{mv^2} \ln\left(\frac{\varepsilon_k}{\varepsilon_k^{\min}}\right)$ describes a braking event in which an electron gives up an energy $> \varepsilon_k^{\min}$, giving rise to REs. In integrating (8), the first term is considered deterministically, and for the second term, a random process is constructed. At the first stage of this process, for REs occurring over a path $\Delta x = v\Delta t$, where Δt is the integration step, the generation of an electron of energy $> \varepsilon_k^{\min}$ is played out. The number of secondary electrons per unit length that can become permanently accelerated is determined as[29–31]

$$\frac{\partial N_{es}}{\partial x} = \sum_a \frac{2\pi e^4 Z_a n_a}{mv^2}\left(\frac{1}{\varepsilon_k^{\min}} - \frac{1}{\varepsilon_k}\right), \tag{10}$$

whence the probability for the generation of an electron is found as

$$P = \sum_a \frac{2\pi e^4 Z_a n_a}{mv^2}\left(\frac{1}{\varepsilon_k^{\min}} - \frac{1}{\varepsilon_k}\right)\Delta x. \tag{11}$$

Next, in the case of a positive outcome, the energy of the generated electron, ε_2', which is in the range $\varepsilon_k^{\min} < \varepsilon_2' < \varepsilon_k$ and is distributed as[31] $\sim 1/(\varepsilon_2')^2$, is played. This is followed by the calculation of the escape angles of the primary and secondary electrons and of the components of their momenta. In our case, we have $\varepsilon_k \gg I_a$, where I_a is the ionization potential of the gas atoms, and the velocity of an incident electron much greater than the orbital electron velocity. Therefore, the collision of a primary electron with an atomic one can be treated as an elastic collision of a fast particle with a particle at rest. Based on this assumption and on the momentum and energy conservation laws, the escape angles are calculated for the primary and the secondary electrons.[32]

The electron-atom collisions are also considered using the Monte Carlo technique. The algorithm is as follows: On each time step, after integration of Eq. (9), a probable collision is played for each particle. In the case of a positive outcome, the scattering angles are calculated using the method described elsewhere.[19]

Relation (10) allows us to estimate the length over which a runaway electron avalanche grows exponentially, l_a. At fields close to E_c, the minimum energy required for an electron to become permanently accelerated can be estimated as[9]

$$\varepsilon_k^{\min} \approx mc^2 \frac{E_c}{2E}. \tag{12}$$

Assuming that $\varepsilon_k \gg \varepsilon_k^{\min}$, in view of (7) and (12), we obtain from (10) a formula to estimate, in the relativistic limit, the characteristic length over which an RE avalanche is generated:

$$l_a^{rel} \approx \left(\frac{\partial N_{es}}{\partial x}\right)^{-1} \approx \frac{mc^2}{eE}\ln\left(\frac{2mc^2}{J}\right). \quad (13)$$

For estimating l_a using (13), the inelastic energy loss J is taken for the most representative gas species, such as nitrogen in air. For a simple estimation of the mean inelastic energy loss for a gas species a, the formula[28] $J_a[eV] \approx 10 + 10Z_a$ can be used.

III. CALCULATION OF THE PARAMETERS OF A RUNAWAY ELECTRON AVALANCHE

The numerical simulation was performed for air with varying gas pressure and E_{av}. The air was assumed to consist of nitrogen (78 wt. %), oxygen (21%), and argon (1%). The calculations were carried out, supposing that at the time zero ($t = 0$), there was one electron with energy $\varepsilon_k = 10\varepsilon_k^{\min}$, up to the occurrence of 10^6–10^8 runaway electrons (N_{es}). An avalanche having passed through a gas leaves an ion "cloud". The parameters of the ion cloud were calculated assuming that the ions were immobile. It should be noted that not all secondary electrons become permanently accelerated. The number of REs in the calculations made 40%–80% of the number of secondary electrons, N_{sec}, depending on the electric field and gas pressure. The electrons with energies $\varepsilon_k < 0.8\varepsilon_k^{\min}$ were eliminated from the calculations together with their nearest ions.

The sought-for quantities were obtained as particle ensemble averages.

First, the spatial characteristics of the avalanche were calculated. The radius vector of the avalanche center point, $\mathbf{R}_{av} \equiv \{X_{av}, Y_{av}, Z_{av}\}$, was found as

$$\mathbf{R}_{av} = \frac{1}{N_{es}}\sum_{i=1}^{N_{es}} \mathbf{R}^i, \quad (14)$$

where $\mathbf{R}^i \equiv \{x^i, y^i, z^i\}$ is the radius vector of the ith runaway electron. Throughout the calculations, the x and y components of the avalanche center radius vector (normal to the electrostatic field) were negligible compared with the z component (Z_{av}) parallel to the field.

The radius vector of the ion cloud center point, $\mathbf{R}_{cl} \equiv \{X_{cl}, Y_{cl}, Z_{cl}\}$, was calculated as

$$\mathbf{R}_{cl} = \frac{1}{N_{ion}}\sum_{i=1}^{N_{ion}} \mathbf{R}_{ion}^i, \quad (15)$$

where $\mathbf{R}_{ion}^i$ is the radius vector of the ith ion and $N_{ion} = N_{es} - 1$ is the number of ions in the cloud. As with the radius vector of the avalanche center point, the x and y components of the radius vector of the ion cloud center point were negligible compared with the z component.

In addition, the rms deviations from the avalanche center point were calculated as

$$\Delta_{||} = \sqrt{\frac{1}{N_{es}}\sum_{i=1}^{N_{es}} (z^i - Z_{av})^2},$$
$$\Delta_{\perp} = \sqrt{\frac{1}{N_{es}}\sum_{i=1}^{N_{es}} \left[(x^i - X_{av})^2 + (y^i - Y_{av})^2\right]}. \quad (16)$$

The quantities $\Delta_{||}$ and $\Delta_{\perp}$ characterize the avalanche dimensions in the directions parallel and normal to the electrostatic field, respectively.

Second, the avalanche characteristics depending on the runaway electron distribution in the velocity domain were determined. The average velocities in the directions parallel and normal to the electrostatic field ($V_{||}$ and $V_{\perp}$, respectively) were found as

$$V_{||} = \frac{1}{N_{es}}\sum_{i=1}^{N_{es}} v_z^i,$$
$$V_{\perp} = \frac{1}{N_{es}}\sum_{i=1}^{N_{es}} \frac{v_x^i(x^i - X_{av}) + v_y^i(y^i - Y_{av})}{\sqrt{(x^i - X_{av})^2 + (y^i - Y_{av})^2}} = \frac{1}{N_{es}}\sum_{i=1}^{N_{es}} v_{\perp}^i, \quad (17)$$

where $\mathbf{v}^i \equiv \left\{v_x^i, v_y^i, v_z^i\right\}$ is the velocity vector of the ith runaway electron.

Third, the energy characteristics of the electron avalanche were calculated. The average kinetic energy of the runaway electrons was found as

$$\bar{\varepsilon}_k = \frac{1}{N_{es}}\sum_{i=1}^{N_{es}} \varepsilon_k^i, \quad (18)$$

where ε_k^i is the kinetic energy of the i-th runaway electron.

The avalanche "temperature" profiles along and transverse to the electrostatic field ($T_{||}$ and $T_{\perp}$, respectively) were calculated using the formulas

$$kT_{||} = \frac{m}{N_{es}}\sum_{i=1}^{N_{es}} \left(v_z^i - V_{||}\right)^2, \quad kT_{\perp} = \frac{1}{2}\frac{m}{N_{es}}\sum_{i=1}^{N_{es}} \left(v_{\perp}^i - V_{\perp}\right)^2, \quad (19)$$

where k is Boltzmann's constant. The factors in (19) were determined proceeding from the fact, known from thermodynamics, that $\frac{1}{2}kT$ is accounted for by each degree of freedom. Certainly, the avalanche "temperatures" bear no relation to actual temperatures; they only characterize the rms deviations from average avalanche velocities.

Finally, the characteristic exponential growth length of an RE avalanche, l_a, and the time of its exponential growth, τ_a, were calculated using the formulas

$$N_{es}^f = N_0 \exp\left\{\left(Z_{av}^f - Z_{av}^0\right)/l_a\right\}; \; N_{es}^f = N_0 \exp\left\{(t_f - t_0)/\tau_a\right\}, \quad (20)$$

where Z_{av}^0 and t_0 are, respectively, the coordinate of the avalanche center point and the time at which the number of REs becomes $N_{es} = N_0$ (in the calculations, $N_0 = 10^4$ was set); Z_{av}^f and t_f are, respectively, the coordinate of the avalanche center point and the time at the end of the calculations (at $N_{es} = N_{es}^f$).

IV. CALCULATED PARAMETERS OF A RUNAWAY ELECTRON AVALANCHE

Figures 1–4 present the results of the simulation of a runaway electron avalanche propagating in air at atmospheric

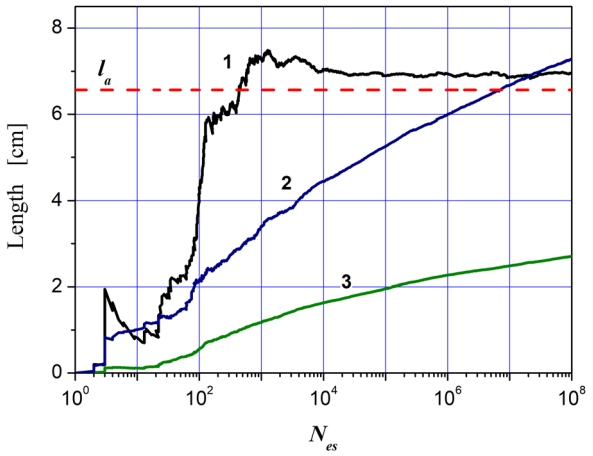

FIG. 1. Dimensions of an RE avalanche in air at a pressure of 1 atm and an electrostatic field of 200 kV/cm versus number of REs: the distance between the avalanche and ion cloud center points, $Z_{av} - Z_{cl}$ (curve 1); the dimension along the field, $\Delta_{||}$ (curve 2), and the dimension transverse to the field, $\Delta_{\perp}$ (curve 3).

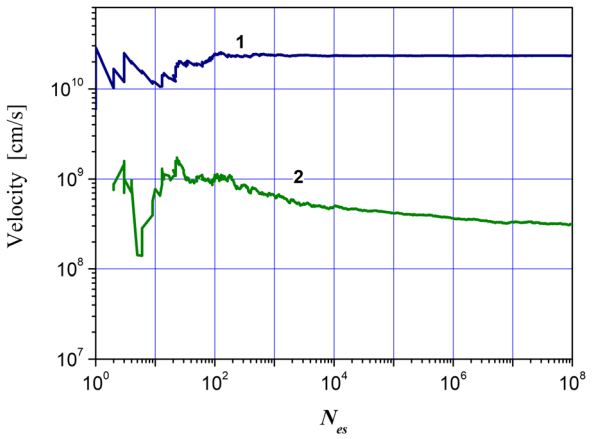

FIG. 2. Velocities of an RE avalanche in air at a pressure of 1 atm and an electrostatic field of 200 kV/cm versus number of REs: the avalanche velocity along the field, $V_{||}$ (curve 1), and transverse to the field, $V_{\perp}$(curve 2).

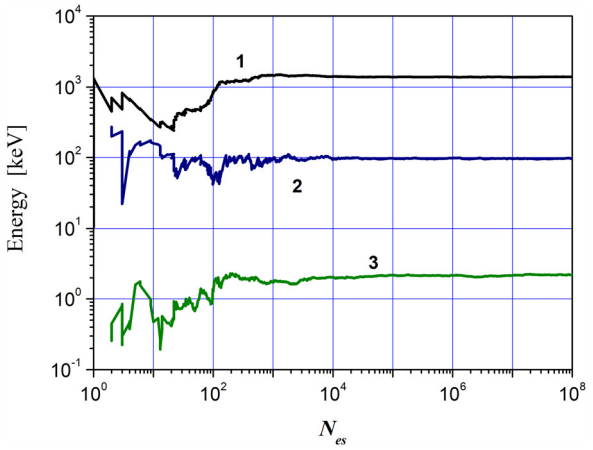

FIG. 3. The average kinetic energy $\bar{\varepsilon}_k$ (curve 1), "temperature" along the field, $T_{||}$ (curve 2), and "temperature" transverse to the field $T_{\perp}$ (curve 3) versus the number of electrons for an RE avalanche at an air pressure of 1 atm and an electrostatic field of 200 kV/cm.

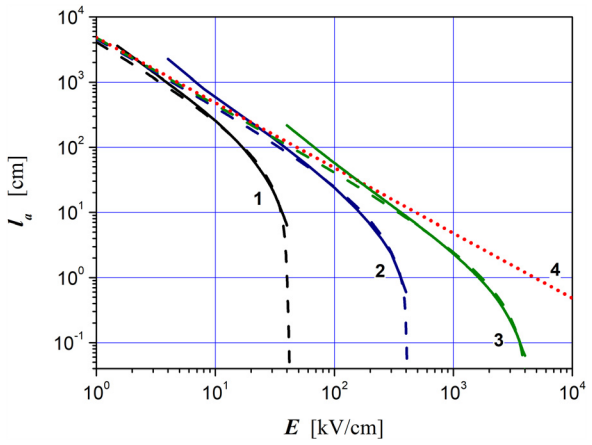

FIG. 4. Characteristic exponential growth length of an RE avalanche at a gas pressure of 0.1 atm (curves 1), 1 atm (curves 2), and 10 atm (curve 3) predicted by the simulation and calculated by (13) (curve 4). Dashed lines depict the curves calculated by (22).

pressure at an electric field strength of 200 kV/cm. The calculations were carried out up to occurring 10^8 runaway electrons in the avalanche. From Figs. 1–3, it can be seen that at the early stage of avalanche propagation (at a small number of REs), the calculated quantities vary irregularly due to transient phenomena. Once the number of REs in the avalanche reaches 10^3–10^4, the transients cease and the variations in avalanche parameters become gradual.

In Fig. 1, the spatial characteristics of the avalanche calculated using formulas (14)–(16) are plotted versus the number of electrons in the avalanche. It can be seen that the characteristic avalanche dimensions along and transverse to the field increase with the number of REs approximately in proportion with $\ln N_{es}$. The distance between the avalanche and ion cloud center points, $Z_{av} - Z_{cl}$, takes a stationary value, which is approximately equal to the exponential growth length of the RE avalanche (for the case under consideration, $l_a \approx 6.6$ cm).

In Fig. 2, the avalanche velocities calculated using formulas (17) are plotted versus the number of electrons in the avalanche. It can be seen that for $N_{es} > 10^3$, the velocity of avalanche propagation along the field, $V_{||}$, takes a stationary value, which, for the given conditions, is $\sim 2.3 \times 10^{10}$ cm/s. The characteristic exponential growth length and time of the avalanche are related with its propagation velocity as

$$\tau_a \approx l_a / V_{||}. \tag{21}$$

Relation (21) is valid to within 1%–2% not only for the given conditions, but also for the gas pressures and electrostatic field strengths considered below.

The existence of the transverse velocity of an avalanche is due to two factors. First, when a fast electron ionizes a gas atom, the velocity vector of the secondary electron is directed almost normal to that of the primary electron (if the energy of the primary electron is substantially greater than that of the secondary one, $\varepsilon'_2 \ll \varepsilon_k$). As the fast electrons travel along the field, the velocity vector of the secondary electrons is originally directed mainly transverse to the field. Second, the elastic scattering of electrons by gas atoms also gives rise to the electron velocity transverse to the field. For

fast electrons, the cross section for elastic scattering is highly nonisotropic,[33] and so, when participating in single collisions, they scatter within small angles. Therefore, the effect of elastic collisions is most pronounced in low electrostatic fields for which the exponential growth length of an RE avalanche is large. As can be seen from Fig. 2, the transverse velocity $V_\perp$ also tends to a stationary value, but, because of the elastic scattering effects, it reaches a stationary value within a longer time than $V_{||}$ does.

Figure 3 presents the energy characteristics of an avalanche calculated using formulas (18) and (19) and plotted versus the number of electrons in the avalanche. It can be seen that when $N_{es} > 10^4$, all avalanche characteristics take stationary values, and we have $\bar{\varepsilon}_k \gg kT_{||} \gg kT_\perp$. This situation is typical for avalanches in strong electric fields; for the fields close to E_c, we have $\bar{\varepsilon}_k \gg kT_{||} \approx kT_\perp$ due to pronounced elastic scattering. The fact that the energy characteristics become stationary indicates that the RE velocity distribution function becomes invariable in form, and only the number of electrons in the avalanche increases.

Thus, as the avalanche propagation velocities, $V_{||}$ and $V_\perp$, and "temperatures," $T_{||}$ and $T_\perp$, and the average kinetic energy of the electrons, $\bar{\varepsilon}_k$, tend to stationary values with increasing number of runaway electrons, these quantities, along with the parameters l_a and τ_a, can be considered characteristics of exponentially growing RE avalanches. Next, we consider how the avalanche parameters depend on gas pressure and electrostatic field strength.

Figure 4 presents the characteristic growth length of an RE avalanche versus the electrostatic field. It can be seen that the curves calculated for low electrostatic fields fit well with formula (13). However, for the fields close to E_{cr}, we see a substantial disagreement, which is related to the occurrence of a significant fraction of nonrelativistic electrons in the avalanche. The disagreement can be eliminated by correcting formula (13) with the use of the relation

$$l_a^{am} \approx l_a^{rel}\left(1 - \sqrt{\frac{E}{E_{cr}}}\right), \tag{22}$$

where l_a^{rel} is the exponential growth length of an RE avalanche, determined by formula (13). The curves calculated using (22) are depicted in Fig. 4 by dashed lines. It can be seen that the approximation by (22) yields good agreement with the simulation predictions.

Figures 5–7 present the spatial characteristics of an RE avalanche versus the electrostatic field for different gas pressures. For all cases, calculations were carried out until the number of runaway electrons in the avalanche reached $N_{es} \approx 10^6$. For comparison, the field dependence of the exponential growth length of an RE avalanche calculated by (22) is plotted for each case.

As can be seen from Figs. 4–7, the distance between the avalanche and ion cloud center points is approximately equal to the exponential growth length of the avalanche, $Z_{av} - Z_{cl} \approx l_a$, for all electrostatic field and pressure values. The avalanche dimensions along and transverse to the field compare in order of magnitude to its exponential growth length, $\Delta_{||} \sim \Delta_\perp \sim l_a$. This holds up to large values of N_{es}. Actually, we have $\Delta_{||} \sim \Delta_\perp \sim \ln N_{es}$; so, if N_{es} increases from 10^6 to 10^{18} (by 12 orders of magnitude), the characteristic dimensions of the avalanche will increase no more than threefold.

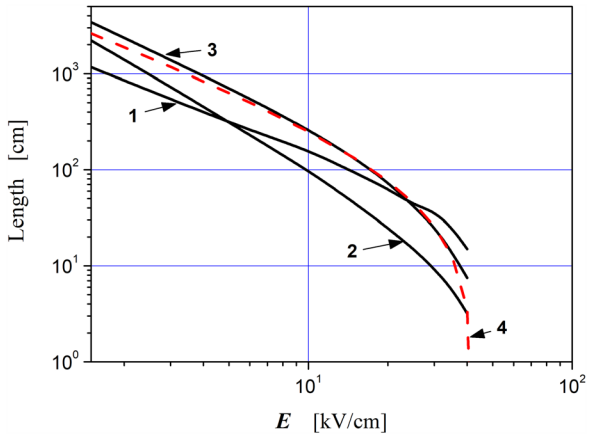

FIG. 5. Electrostatic field dependences of the avalanche dimensions for $N_{es} \approx 10^6$ and 0.1 atm gas pressure: $\Delta_{||}$ (curve 1), $\Delta_\perp$ (curve 2), and $Z_{av} - Z_{cl}$ (curve 3), and of the avalanche exponential growth length calculated by (22) (curve 4).

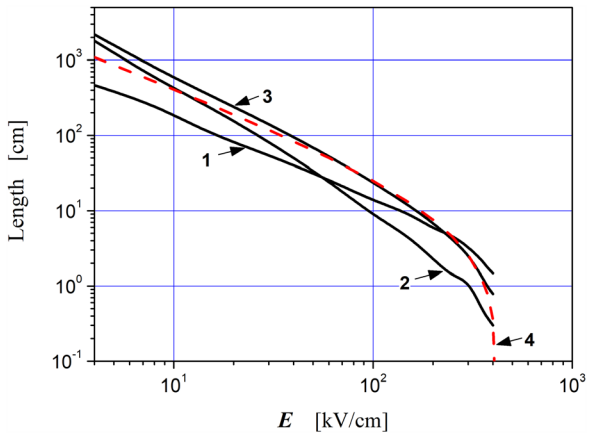

FIG. 6. Electrostatic field dependences of the avalanche dimensions for $N_{es} \approx 10^6$ and 1 atm gas pressure: $\Delta_{||}$ (curve 1), $\Delta_\perp$ (curve 2), and $Z_{av} - Z_{cl}$ (curve 3), and of the avalanche exponential growth length calculated by (22) (curve 4).

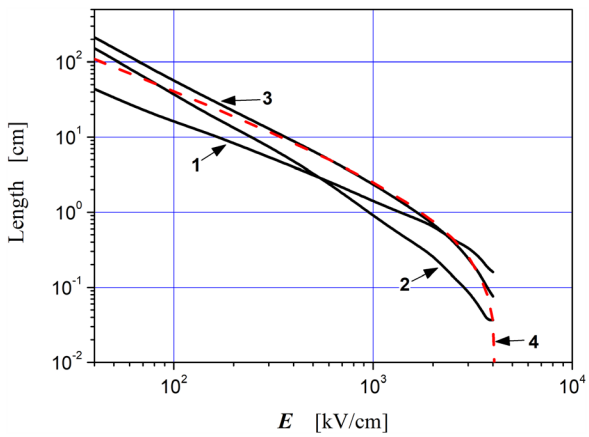

FIG. 7. Electrostatic field dependences of the avalanche dimensions for $N_{es} \approx 10^6$ and 10 atm gas pressure: $\Delta_{||}$ (curve 1), $\Delta_\perp$ (curve 2), and $Z_{av} - Z_{cl}$ (curve 3), and of the avalanche exponential growth length calculated by (22) (curve 4).

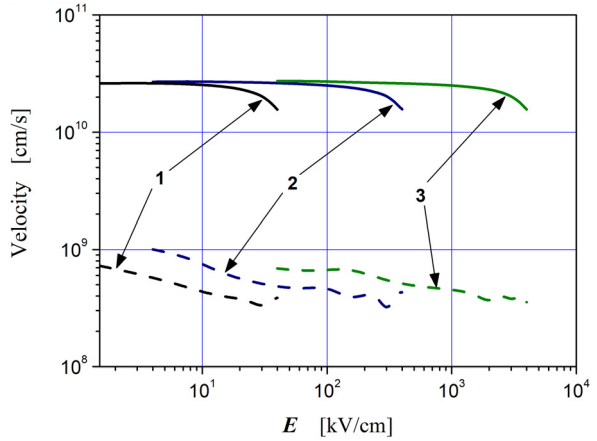

FIG. 8. Electrostatic field dependences of the velocities of an RE avalanche along the field, $V_{||}$ (solid lines), and transverse to the field, $V_{\perp}$ (dashed lines), at different gas pressures: 0.1 atm (curves 1), 1 atm (curves 2), and 10 atm (curves 3).

Figure 8 presents the velocities of an RE avalanche versus electrostatic field for different gas pressures, and Fig. 9 presents the respective field dependence of the average kinetic energy of the runaway electrons in the avalanche, $\bar{\varepsilon}_k$.

As can be seen from Fig. 8, the both velocities, $V_{||}$ and $V_{\perp}$, are maximal at an electric field close to E_c, $V_{||}$ reaching 2.7×10^{10} cm/s and $V_{\perp}$ being two orders of magnitude lower than $V_{||}$. The velocity sharply decreases as soon as the electrostatic field approaches its critical value E_{cr} (in the simulation, the minimum $V_{||}$ was about 1.5×10^{10} cm/s). As the condition $\varepsilon_k \gg I_a$ (I_a is the ionization potential of the gas atoms) is poorly fulfilled when the braking force approaches a maximum, the method used to simulate RE avalanches is of limited utility for the electric fields $E \approx E_{cr}$. Therefore, the calculations were carried out up to $E = 0.95 \cdot E_{cr}$; so, it is quite probable that the values of $V_{||}$ at $E \to E_{cr}$ could be substantially lower than those presented in Fig. 8. The average kinetic energy of the avalanche REs also sharply decreases as soon as the electric field strength approaches E_{cr}. For low field strengths close to E_c, we have $\bar{\varepsilon}_k \approx 5$ MeV, i.e., $\bar{\varepsilon}_k \approx \varepsilon_{\min}$, where $\varepsilon_{\min}$, determined by formula (6), is the

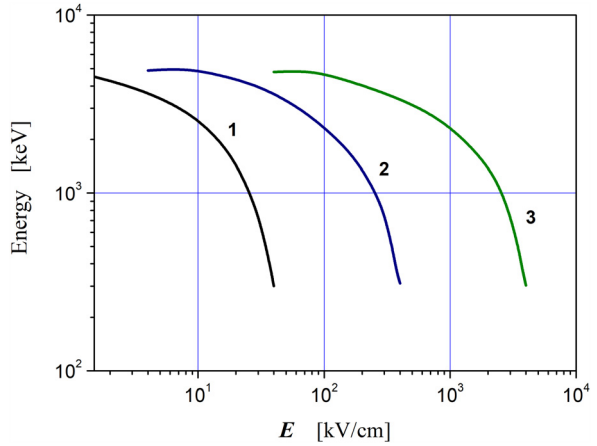

FIG. 9. Electrostatic field dependence of the average kinetic energy of the runaway electrons in an avalanche, $\bar{\varepsilon}_k$, for different gas pressures: 0.1 atm (curves 1), 1 atm (curves 2), and 10 atm (curves 3).

electron energy corresponding to the minimum braking force (see formula (1)).

The results above refer to a situation in which the space charge created by the REs and ion cloud does not affect the avalanche development, i.e., when N_{es} is relatively small. As the electrons and ions increase in number, the space charge field becomes comparable to the applied electrostatic field, resulting in cessation of the exponential growth of REs in the avalanche. This situation is similar to the so-called avalanche-to-streamer transition in ordinary electron avalanches[34–36] that occurs when an avalanche propagates the distance

$$Z_e^{cr} \approx \frac{1}{\alpha} \ln N_e^{cr}, \tag{23}$$

where α is the Townsend ionization coefficient and N_e^{cr} is the critical number of electrons in the avalanche. The quantity N_e^{cr} depends intricately on the electric field and on the gas species and pressure.[37] It is conventionally assumed that[37] $N_e^{cr} \approx (1\text{–}5) \times 10^8$.

For an RE avalanche, we can determine the distance the avalanche has propagated until its behavior becomes critical as

$$Z_{es}^{cr} \approx l_a \ln N_{es}^{cr}, \tag{24}$$

where N_{es}^{cr} is the number of REs at which the space charge field becomes comparable to the applied electrostatic field. Thus, the exponential growth length of an RE avalanche, l_a, is analog to the ionization coefficient α.[9,13]

By analogy with an ordinary avalanche,[34–36] the critical number of electrons in an RE avalanche can be estimated by comparing the space charge field with the applied electrostatic field by using the relation

$$\frac{eN_{es}^{cr}}{\Delta_{\perp}^2} \approx E, \tag{25}$$

where $\Delta_{\perp}$ is the avalanche dimension transverse to the field.

Then, the critical pulse current and current density of runaway electrons in the avalanche can be estimated as

$$I_{es}^{cr} \approx \frac{v_{||} e N_{es}^{cr}}{2\Delta_{||}} \approx v_{||} E \frac{\Delta_{\perp}^2}{2\Delta_{||}}; \quad j_{es}^{cr} = \frac{I_{es}^{cr}}{\pi \Delta_{\perp}^2} \approx \frac{v_{||} E}{2\pi \Delta_{||}} \tag{26}$$

where $v_{||}$ and $\Delta_{||}$ are, respectively, the avalanche velocity and dimension along the field for the pulse duration determined as

$$\tau_{es}^{cr} \approx \frac{eN_{es}^{cr}}{I_{es}^{cr}} = \frac{2\Delta_{||}}{v_{||}}. \tag{27}$$

As mentioned (see Figs. 5–7), the characteristic dimensions of an avalanche along and transverse to the field are close to its exponential growth length l_a. Therefore, using (14) and (23), we obtain the following formula for the critical number of electrons in an RE avalanche:

$$N_{es}^{cr} \approx \frac{m^2 c^4}{e^3} \frac{a^2}{E} \left[\left(1 - \sqrt{\frac{E}{E_{cr}}} \right) \ln \left(\frac{2mc^2}{J} \right) \right]^2, \tag{28}$$

where $a = \Delta_\perp / l_a^{am}$ is a dimensionless coefficient of order unity.

The critical pulse current in an RE avalanche (at the point in space where the avalanche has grown to its critical size) can be estimated as

$$I_{es}^{cr} \approx I_A \frac{v_{||}}{c} \frac{a^2}{2b} \left(1 - \sqrt{\frac{E}{E_{cr}}}\right) \ln\left(\frac{2mc^2}{J}\right), \tag{29}$$

where $I_A = \frac{mc^3}{e} \approx 17\,\text{kA}$ is the Alfven current and $b = \Delta_{||} / l_a^{am}$ is a dimensionless coefficient of order unity.

RE avalanches seem to play a significant part in two limiting cases. These are, first, high-altitude atmospheric air discharges[8,9] in which the average electrostatic fields are close to E_c and, second, gas discharges in overvolted electrode gaps[21–26] in which the average electrostatic fields are close to E_{cr}. Let us estimate the critical parameters of an avalanche developing in air at atmospheric pressure for these cases.

For electrostatic fields close to E_c, i.e., to the minimum field at which electrons can run away, the dimensionless coefficients can be estimated as $a \approx 3$ and $b \approx 1$. Then, we obtain the following estimates for the critical number of REs in an avalanche propagating in air at atmospheric pressure with $E \approx 3\,\text{kV/cm}$, according to (28), $N_{es}^{cr} \approx 4 \times 10^{17}$; for the critical parameters of the current pulse in the avalanche: $I_{es}^{cr} \approx 600\,\text{kA}$, $j_{es}^{cr} \approx 0.01\,\text{A/cm}^2$, and $\tau_{es}^{cr} \approx 100\,\text{ns}$, and for the distance propagated by the avalanche until its behavior becomes critical $Z_{es}^{cr} \approx 600\,\text{m}$. This Z_{es}^{cr} is substantially smaller than the characteristic dimensions of high-altitude atmospheric discharges that can be as long as several tens of kilometers.[8,9]

For $E \to E_{cr}$, we have $a \approx 0.3$ and $b \approx 3$ (see Figs. 5–7). In this case, as follows from (22) and (28), l_a and N_{es}^{cr} both tend to zero. However, the critical number of electrons in an RE avalanche, N_{es}^{cr}, cannot be smaller than the critical number of electrons in an ordinary avalanche, N_e^{cr}; that is, we can assume that $N_{es}^{cr} \approx N_e^{cr}$. Then, using (25), we obtain an approximate formula for estimating the avalanche exponential growth length for this case: $l_a \approx \frac{1}{a}\sqrt{\frac{eN_e^{cr}}{E_{cr}}}$. Using (26), we can estimate the critical current amplitude for an RE avalanche with $E \to E_{cr}$ as $I_{es}^{cr} \approx \frac{a^2}{2b} v_{||} E_{cr} l_a$. The velocity of electrons in an avalanche (in a nonrelativistic case) cannot be greater than $v_{||} = \sqrt{\frac{2eE_{cr}l_a}{m}}$, and, hence, we have $I_{es}^{cr} \approx \left(\frac{e^5}{4m^2}\right)^{1/4} \frac{\sqrt{a}}{b} \left(N_e^{cr} E_{cr}\right)^{3/4}$. Putting for air at atmospheric pressure $E_{cr} \approx 420\,\text{kV/cm}$ and assuming that $N_e^{cr} \approx 10^8$, we obtain the following estimates for the RE avalanche critical parameters: $l_a \approx 2 \times 10^{-2}\,\text{cm}$, $I_{es}^{cr} \approx 0.75\,\text{A}$, $j_{es}^{cr} \approx 7 \times 10^3\,\text{A/cm}^2$, $\tau_{es}^{cr} \approx 20\,\text{ps}$, and $Z_{es}^{cr} \approx 0.36\,\text{cm}$.

To conclude, we should make a remark on the similarity laws applied to gas discharges. They manifest themselves in that the discharge parameters depend on the ratio $\left(\frac{E}{p}\right)$ rather than on electric field E and pressure p individually.[10,37,38] It is well known[37] that the Townsend ionization coefficient obeys the similarity law $\frac{\alpha}{p} \sim f\left(\frac{E}{p}\right)$. A similarity law can also be formulated for the exponential growth length of an RE avalanche as for the analog to the Townsend ionization coefficient. As the critical field is determined only by the gas species and pressure, in view of (13) and (22), the similarity law for RE avalanches can be written as $l_a E \approx \frac{mc^2}{e}\left(1 - \sqrt{\frac{E}{E_{cr}}}\right) \ln\left(\frac{mc^2}{J}\right) \sim f\left(\frac{E}{p}\right)$. The plots in Figs. 8 and 9 indicate that other parameters of an RE avalanche ($V_{||}$, $V_\perp$, and $\bar{\varepsilon}_k$) also depend on $f\left(\frac{E}{E_{cr}}\right) \sim f\left(\frac{E}{p}\right)$; that is, they also obey similarity laws.

V. CONCLUSIONS

The features of runaway electron avalanches developing in air have been investigated for different air pressures using a three-dimensional numerical simulation. The numerical model took into account the electron braking due to inelastic energy loss, the elastic scattering of electrons by the gas atoms, and the generation of secondary electrons. The simulation results have shown that an RE avalanche can be characterized, besides the time and length of its exponential growth, by the propagation velocity and by the average kinetic energy of the runaway electrons. The relations of these parameters to the gas pressure and applied electrostatic field have been found. It has been shown that the parameters of an RE avalanche obey the similarity laws applied to gas discharges.

ACKNOWLEDGMENTS

The work was supported by the Russian Foundation for Basic Research Grant No. 16-38-60199; Scholarship of the President of the Russian Federation Grant No. SP-951.2016.1.

[1]S. Frankel, V. Highland, T. Sloan, O. Vandyck, and W. Wales, Nucl. Instrum. Methods **44**(2), 345 (1966).
[2]Y. L. Stankevich and V. Kalinin, Sov. Phys. Doklady **12**, 1042 (1968).
[3]R. C. Noggle, E. P. Krider, and J. R. Wayland, J. Appl. Phys. **39**(10), 4746 (1968).
[4]G. K. Parks, B. H. Mauk, R. Spiger, and J. Chin, Geophys. Res. Lett. **8**(11), 1176–1179, doi:10.1029/GL008i011p01176 (1981).
[5]M. McCarthy and G. K. Parks, Geophys. Res. Lett. **12**(6), 393–396, doi:10.1029/GL012i006p00393 (1985).
[6]A. V. Gurevich, G. M. Milikh, and R. Rousseldupre, Phys. Lett. A **165**(5-6), 463–468 (1992).
[7]N. G. Lehtinen, U. S. Inan, and T. F. Bell, Geophys. Res. Lett. **27**(8), 1095–1098, doi:10.1029/1999GL010765 (2000).
[8]V. P. Pasko, Nature **423**(6943), 927–929 (2003).
[9]A. V. Gurevich and K. P. Zybin, Phys.-Usp. **44**(11), 1119–1140 (2001).
[10]Y. D. Korolev and G. A. Mesyats, *Physics of Pulsed Breakdown in Gases* (Nauka, Moscow, 1991).
[11]M. M. Tsventoukh, V. G. Mesyats, and S. A. Barengolts, Plasma Fusion Res. **5**, S2069 (2010).
[12]V. F. Tarasenko and S. I. Yakovlenko, Phys.-Usp. **47**(9), 887 (2004).
[13]L. Babich, E. Donskoy, R. Il'kaev, A. Y. Kudryavtsev, I. Kutsyk, and B. Shamraev, Doklady Phys. **46**(8), 536–539 (2001).
[14]J. R. Dwyer, Phys. Plasmas **14**(4), 042901 (2007).
[15]D. Levko, V. T. Gurovich, and Y. E. Krasik, J. Appl. Phys. **110**(4), 043302 (2011).
[16]D. Levko, V. F. Tarasenko, and Y. E. Krasik, J. Appl. Phys. **112**, 073304 (2012).
[17]S. Y. Belomyttsev, I. V. Romanchenko, V. V. Ryzhov, and V. A. Shklyaev, Tech. Phys. Lett. **34**(5), 367–369 (2008).
[18]E. V. Oreshkin, S. A. Barengol'ts, A. V. Oginov, V. I. Oreshkin, S. A. Chaikovskii, and K. V. Shpakov, Tech. Phys. Lett. **37**(6), 582–585 (2011).
[19]E. V. Oreshkin, S. A. Barengolts, S. A. Chaikovsky, and V. I. Oreshkin, Phys. Plasmas **19**(4), 043105 (2012).

[20]V. Oreshkin, E. Oreshkin, S. Chaikovsky, and A. Artyomov, Phys. Plasmas **23**(9), 092701 (2016).
[21]A. V. Gurevich, G. A. Mesyats, K. P. Zybin, A. G. Reutova, V. G. Shpak, S. A. Shunailov, and M. I. Yalandin, Phys. Lett. A **375**(30-31), 2845–2849 (2011).
[22]V. F. Tarasenko, S. A. Shunailov, V. G. Shpak, and I. D. Kostyrya, Laser Particle Beams **23**(4), 545–551 (2005).
[23]G. A. Mesyats, S. D. Korovin, K. A. Sharypov, V. G. Shpak, S. A. Shunaillov, and M. I. Yalandin, Tech. Phys. Lett. **32**(1), 18–22 (2006).
[24]G. A. Mesyats and M. I. Yalandin, IEEE Trans. Plasma Sci. **37**(6), 785–789 (2009).
[25]G. A. Mesyats, A. G. Reutova, K. A. Sharypov, V. G. Shpak, S. A. Shunailov, and M. I. Yalandin, Laser Part. Beams **29**(4), 425–435 (2011).
[26]M. I. Yalandin, G. A. Mesyats, A. G. Reutova, K. A. Sharypov, V. G. Shpak, and S. A. Shunailov, Tech. Phys. Lett. **37**(4), 371–375 (2011).
[27]E. V. Oreshkin, S. A. Barengolts, S. A. Chaikovsky, A. V. Oginov, K. V. Shpakov, and V. A. Bogachenkov, Phys. Plasmas **19**(1), 013108 (2012).
[28]L. D. Landau and E. M. Lifshits, *Quantum Mechanics* (Nauka, Moscow, 1988).
[29]E. V. Oreshkin, S. A. Barengolts, V. I. Oreshkin, and S. A. Chaikovsky, Tech. Phys. Lett. **38**(7), 604–608 (2012).
[30]E. Oreshkin, S. Barengolts, S. Chaikovsky, and V. I. Oreshkin, Phys. Plasmas **22**(12), 123505 (2015).
[31]L. D. Landau, J. Bell, M. Kearsley, L. Pitaevskii, E. Lifshitz, and J. Sykes, *Electrodynamics of Continuous Media* (Elsevier, 1984).
[32]L. D. Landau and E. M. Lifshits, *The Classical Theory of Fields* (Fizmatgiz, Moscow, 1959).
[33]M. Mitchner and C. H. Kruger, *Partially Ionized Gases* (Jhon Willey and Sons, New York, 1973).
[34]L. B. Loeb, *Fundamental Processes of Electrical Discharge in Gases* (J. Willey and Sons, New York, 1939).
[35]J. Meek and J. Craggs, Electrical breakdown of gases, Oxford (1953).
[36]H. Raether, *Electron Avalanches and Breakdown in Gases* (Butterworths, London 1964).
[37]G. A. Mesyats, Y. I. Bychkov, and V. Kremnev, Phys.-Usp. **15**(3), 282–297 (1972).
[38]G. A. Mesyats, Phys.-Usp. **49**(10), 1045 (2006).